Engineered Science
DOI: https://dx.doi.org/10.30919/es1589

Automated Production of 3D Printed Concrete Structures with Integrated Reinforcement Mesh Based on Standard Reinforcement Bars

Mukhagali Sagyntay,[1, 2,*] Florian Storch,[3, 4,*] Azamat Mustafa,[1, 2,*] Paul Plaschnick,[3] Frank Will[3, 4] and Zhumadil Baigunchekov[5]

Abstract

3D concrete printing is developing rapidly and is seen as an alternative to traditional construction methods. But today, the use of standard steel reinforcements and their integration into the concrete is very relevant for 3D concrete printing. The currently available measures provide the automated production of the reinforcement mesh but the concreting is manual, or automates both the creation of the reinforcement mesh and concreting but the integration of the reinforcement into the concrete is not sufficient to meet the requirements regarding strength and durability. To fill this gap, this study proposes a novel concept that automates the creation of reinforcement mesh and its integration into concrete during the 3D printing process. To verify the feasibility of the concept, tests were carried out: a mesh strength test according to DIN 488-4, an X-ray scanning test for the integration of the reinforcement mesh into concrete, and a cross-section cut test perpendicular to the printing direction and in line with the printing direction. The results show that the proposed concept is viable.

Keywords: 3D concrete printing, standard steel reinforcement, reinforcement mesh, nozzle, integration zone.
Received: 25 March 2025; Revised: 29 May 2025; Accepted: 10 June 2025.
Article type: Research article.

1. Introduction

Additive technology is revolutionizing the construction industry, with 3D concrete printing being the most common application. By application of this method, building constructions with cement-based concrete mixes are automated in a predefined digital path. The 3D concrete printing can provide design flexibility by minimizing material waste and improving sustainability. It also effectively reduces construction period and labor requirements by increasing site safety and significantly reducing the overall costs.[1] For example, the technology makes it possible to save 30-60 % of the material, reduce waste and build 50-80 % faster.[2] To date, many issues have been researched regarding the 3D concrete printing process, such as rheology,[3-5] pumpability and extrudability,[6-8] printing speed,[9] interlayer bonds,[10-14] and economic or environmental impact.[15,16]

Currently, the biggest technological hurdle in 3D concrete printing is the efficient in-process method of reinforcement integration.[17] To become one of the main construction methods in the future, it is imperative to automate the process of reinforcement integration. To facilitate the automation of the reinforcement process, materials such as cables and chains,[18-24] metal fibers, short rods and staples,[25-28] metal mesh,[29] screws and robotic welding of vertical reinforcement have been studied in previous research works.[30-33] Although these methods allow for the automation of the process of reinforcement, reinforced concrete produced by these methods can not be an adequate alternative to the traditional method, because they are not comparable with the standard steel reinforcement in terms of mechanical characteristics. The use of standard steel reinforcement increases the mechanical performance of 3D-printed concrete, making it comparable to conventionally produced reinforced concrete.[34-36] However, in these works the reinforcement was laid by hand as reported in literature for before,[37-39] during or after the concrete

[1] *Department of Mechanical Engineering, Satbayev University, Almaty, 050013, Kazakhstan*
[2] *RnD Center LLP, Almaty, 050013, Kazakhstan*
[3] *Chair of Construction Machinery, TUD Dresden University of Technology, Dresden, 01187, Germany*
[4] *Construction Future Lab gGmbH, Dresden, 01069, Germany*
[5] *Department of Mechanics, Al-Farabi Kazakh National University, Almaty, 050040, Kazakhstan*
**E-mail:* mukhagali.sagyntay@gmail.com (M. Sagyntaya);
florian.storch@tu-dresden.de (F.Storch);
a.mustafa@satbayev.university (A. Mustafa)

printing.[40-47] Detailed information on reinforcement strategies and methods.[48]

The process of automatic reinforcement with standard steel reinforcement by introducing vertical short standard steel reinforcements perpendicular to the printing direction has been investigated.[49,50] But the integration of reinforcement into concrete was only possible by dipping the reinforcement into a special paste or by screwing it into concrete. Meanwhile, these methods are only able to reinforce in vertical directions. And also studied the possibility of reinforcement in horizontal direction by introducing short standard steel reinforcement bars between the layers.[51] Although welded horizontal and vertical reinforcing bars are used in this work, the vertical reinforcing bars are very short and the possibility of connecting horizontal reinforcing bars located at different heights with vertical reinforcing bars was not even considered. In the concept of Mesh Mould developed by researchers at ETH Zurich, the process of making reinforcement mesh from standard steel reinforcement rods is maximally automated, but the process of concreting is done manually, and there is no possibility to use concrete with similar compositions and characteristics to traditional concrete.[52] Classen *et al.* proposed to reinforce both in vertical and in horizontal directions during printing by joining using the process of arc welding segmented steel reinforcement bars into a three-dimensional reinforcement mesh and simultaneously pouring with extruded concrete.[53,54] In the proposed concept, the horizontal and vertical segments are welded together at the butt joint to form long bars. At the junction point between the horizontal and vertical, bars are not connected to each other but only arranged in a crossing manner, which does not allow for the redistribution of the load between the horizontal and vertical bars efficiently. Also, the physical separation of the nozzles resulted in poor integration of the reinforcing bars into the concrete.

In order to approach the level of automation of the reinforcement process proposed in the Mesh Mould concept, and to eliminate the disadvantage of the concept proposed by Classen et al. in the form of poor integration of reinforcement bars into the concrete, as well as manually pouring of concrete, this paper proposes a new concept. In brief, both the concrete printing process and the reinforcement process are automated as much as possible, and a solution to the problem of integration of reinforcement bars into the concrete during printing is proposed through an integration zone in the nozzle. In order to automate the reinforcement process, a prototype automatic reinforcing mechanism was designed and fabricated to produce reinforcement meshes from standard 8 mm diameter steel reinforcement by joining horizontal and vertical reinforcement by spot contact welding. Shear tests were performed according to DIN EN ISO 15630-2 to determine the strength of the welded joints of the reinforcement mesh, and the results were compared with the minimum node strength in accordance with DIN 488-4. In order to integrate the reinforcement mesh into the concrete during printing, a special nozzle with an integration zone was designed and manufactured. To demonstrate the effect of the integration zone in the nozzle, a sample was 3D printed, where the integration zone is preserved in the first and second layers, and is intentionally broken in the third layer. To verify the integration of the reinforcement mesh into the concrete, the specimen was first scanned by X-ray and then cut lengthwise and crosswise for visual inspection.

2. Materials

2.1 Printed concrete

The printable mix is a concrete with a coarse aggregate. While in most concrete printing, researchers work with fine-grained mortar with a maximum grain size of 2 mm. The maximum grain size in the tests reported here is 16 mm, thus representing the worst case with regard to the uniform distribution of the concrete around the reinforcement bars. Table 1 shows the proportions of the individual components. This mixture was used in all tests with concrete. The used 3D printed mixture has been successfully implemented and described in previously published papers.[55]

Table 1: Concrete components of the mixture used in the tests.

No	Components	Mass [kg/m³]
1	CEM II/C-M (S-LL)	464.0
2	Silica sand BCS 413	136.5
3	Sand 0/2	516.4
4	Gravel 2/4	286.6
5	Gravel 4/8	266.5
6	Gravel 8/16	415.1
7	Water	208.8
8	Superplasticizer	as required

The production process for the concrete mix is as follows: The dry components, such as cement, silica sand, sand and gravel, were thoroughly mixed in a mixer for 2 minutes. Then, water was gradually added while continuously mixing and the continuous mixing process was monitored for 3-4 min. If necessary, a superplasticizer was added to the concrete to reduce the consistency while maintaining the same water/cement ratio and to simplify workability without significantly affecting the hardened concrete properties.

2.2 Steel reinforcement

For the production of the reinforcing mesh, a standard steel bar was selected in accordance with DIN 488-1:2009-08. The selected diameter of a bar is 8 mm, as this bar is widely used in the construction industry and the energy required for resistance spot welding remains limited in the initial phase for a proof of concept. The ribbing of the bars is standardized and improves the force transmission between concrete and steel.

3. Methods

3.1 Creation of a reinforcement mesh from standard steel reinforcement bars using resistance spot welding

3.1.1 The reinforcement mesh

In the traditional method of pouring reinforced concrete, conventional reinforcement meshes (frames) consist of reinforcement bars located vertically (z), horizontally (x) and in depth (y) and they are connected to each other by knitting wire or welding. From the design features, each of these reinforcement bars provides strength in the corresponding directions. In most cases, the main ones are vertical reinforcement bars that perceive tensile-compressive loads, whose diameter is larger than in other directions. But it is impossible to repeat the same configuration of reinforcement meshes in 3D printed concrete at this stage of its development due to the peculiarities of this technology. The essence of the technology of 3D printing concrete is the layer-by-layer pouring of concrete in the horizontal (conditionally) direction, and the structure is "built up" in the vertical direction after each poured layer. Accordingly, there is a high risk of the nozzle hitting the vertical reinforcement bars if they are installed as in the traditional method of pouring reinforced concrete. This means that the reinforcement mesh should also be "built up" gradually during 3D printing. In this case, at this stage of development of 3D concrete printing technology, it is not possible to keep the vertical reinforcement bars whole and long (for effective resistance to tensile-compressive forces), you will have to divide them into pieces of a certain length and assemble them during 3D printing. Below is one of the options for creating a reinforcement mesh for 3D printed concrete during 3D printing.

The creation of the reinforcing mesh was carried out by resistance welding of vertical and horizontal reinforcing bars with a diameter of 8 mm in two rows. As shown in Fig. 1A, each row of the reinforcing mesh consists of several horizontal reinforcements arranged parallel in height with an interaxial distance of 50 mm. Vertical reinforced bars are staggered with an interaxial distance of 150 mm, so that the interaxial distance between the vertical bar of the current layer and the vertical bar of the previous layer will be 75 mm (Fig. 1B).

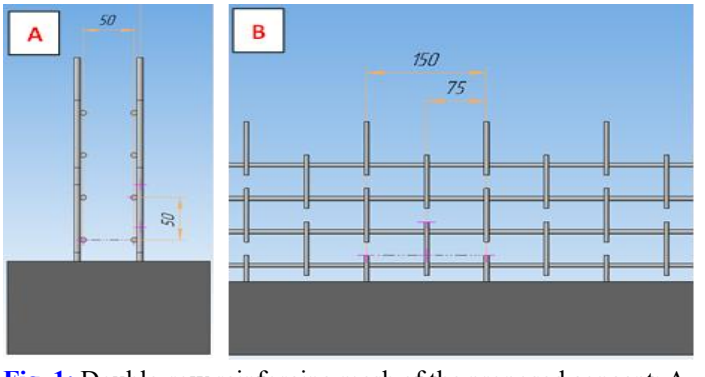

Fig. 1: Double-row reinforcing mesh of the proposed concept: A-reinforcing mesh cross section and B-reinforcing mesh front view.

At this stage of the proposed concept, the two rows of reinforcement meshes are not connected to each other as is usually the case in reinforcement meshes (frames) of a traditional reinforced concrete structure. Since this work studies the possibility of creating a reinforcement mesh from standard steel reinforcement bars during 3D printing in automatic mode and integrating the created reinforcement mesh into 3D printed concrete.

3.1.2 Creating a reinforcement mesh using the automatic reinforcement mechanism

To automate the process of reinforcement manufacturing and reinforcement integration during 3D printing of concrete, the concept of an automatic reinforcing mechanism was created, designed, produced and tested. Fig. 2A shows its simplified scheme: The speed of the nozzle V_{CN} is equal to the speed of the platform (Frame of the reinforcing mechanism) $V_{PLATFORM}$, since it has a rigid connection with the printhead. In front of the platform, there is a horizontal bars feeder which is responsible for positioning horizontal reinforcing bars at a certain height and ensure immobility relative to the ground during welding. From inside of the platform, there is a magazine of two rows, where there is a certain number of vertical reinforcing bars. The vertical bars feeder is located under the magazine and is liable to transfer the vertical bars from the magazine to the welding system. The platform has a moving system that ensures that the electrodes remain stationary relative to the horizontal reinforcing bars during welding. On the moving system, there is a welding system with electrodes where the moving system moves back relative to the platform at a speed V_{COMP} during welding. After the end of the welding, it returns the electrodes at a speed V_{BACK} to its original position under the vertical bar feeder. The optional cooling system cools the weld seams until the temperature falls below the maximum permissible temperature for concrete installation and the nozzle coats the welded reinforcing bars with concrete. Figs 2B and C show the first prototype and prototype testing images.

The operating principle of the autonomic mechanism for the reinforcement manufacturing and integration is as follows: The horizontal feeder moves the reinforcement bars into the welding zone. The bars run parallel at a distance of 50 mm with a length of 1-2 m. Before the printing process, the magazine was loaded with vertical bars. These are 80 mm long and also arranged in two parallel rows. The vertical bar feeder discloses the bars from the magazine and positions them in the welding zone. The electrode clamps the horizontal and vertical bars in the welding zone. Then the two rows of reinforcement are welded simultaneously (welding time approx. 0.3-0.5 s).[56] The electrode remains stationary during the welding process and moves back in relation to the direction of printing, allowing the printing process to continue uninterrupted. After welding, the electrodes open and the welding unit quickly returns to the home position. At the same time, the spot weld passed through the cooling system and was cooled down. The concrete nozzle, which is located behind the reinforcement integration mechanism, prints the current concrete layer and encloses the reinforcement with concrete.

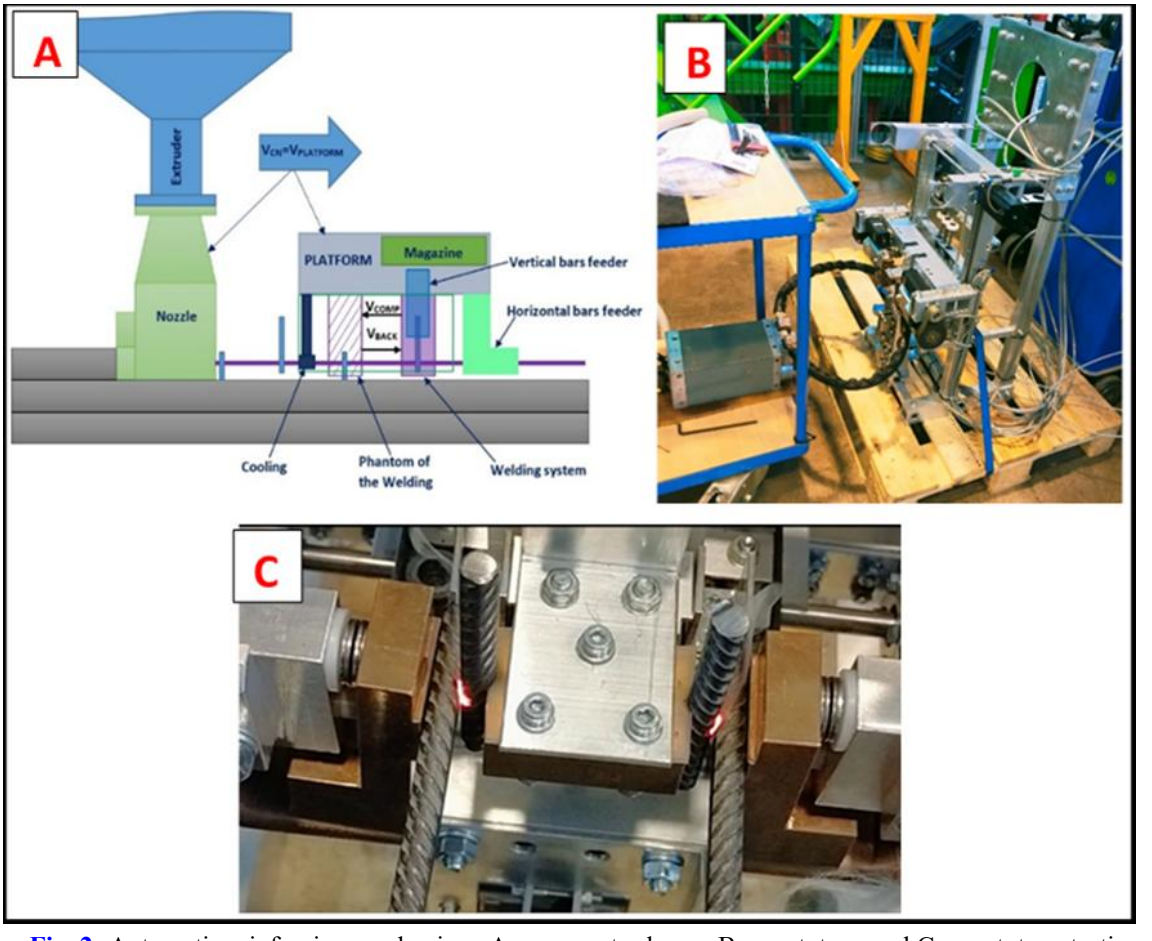

Fig. 2: Automatic reinforcing mechanism: A – concept scheme, B – prototype and C – prototype testing.

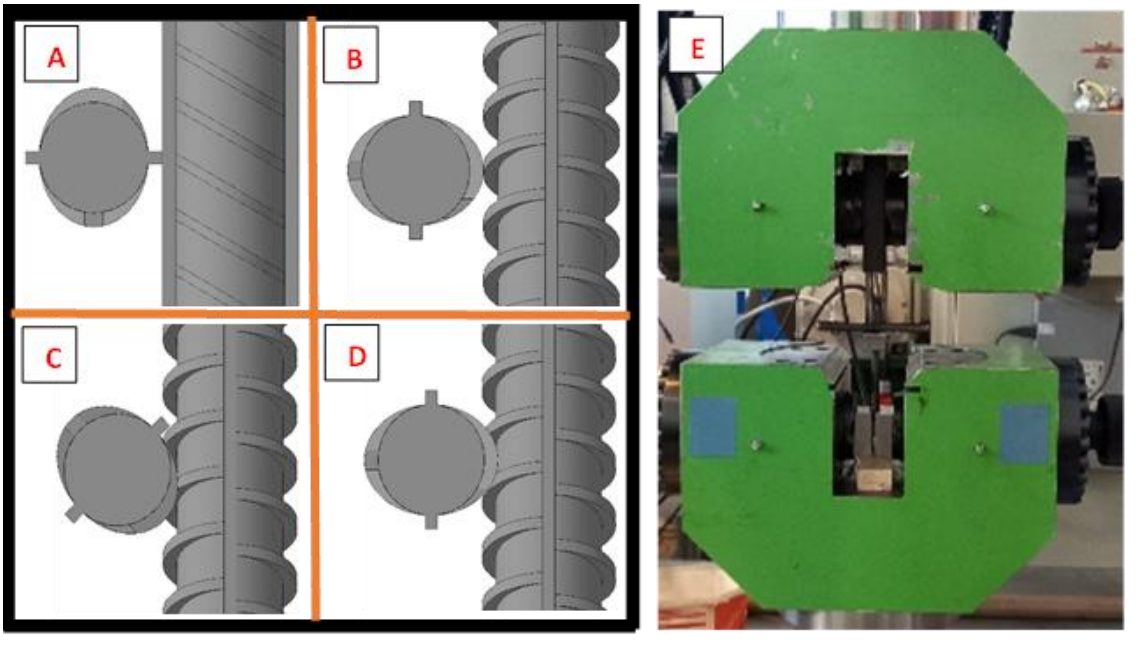

Fig. 3: The location of the reinforcing bars relative to each other in different combinations and test setup for shear tests: A – edge/edge; B – rib/rib, C – pocket/pocket; D – rib/pocket; E - shear tests on crossing specimens.

3.1.3 Contact welding parameters and preliminary tests

For the connection of vertical and horizontal reinforcement, the resistance spot welding method was chosen, since it is widely used in the production of reinforcing meshes and, most importantly, this method is fully standardized and described in the DIN EN ISO 17660-1 standard. Therefore, only the

compliance with this standard needs to be achieved. Samples were made where the reinforcing bars were located relative to each other in different combinations: edge to edge, rib to rib, pocket to pocket, rib to pocket (Figs. 3A-D). In all cases, the reinforcing bars were placed crosswise at 90 degrees and connected using the automatic reinforcing mechanism. For each combination, 5 specimens were made and shear tested in a servo-hydraulic testing system as shown in Fig. 3E, with a constant load rate of 800 kN/s according to DIN EN ISO 15630-2. For all tests the welding time was 0.3 s and the compression force of the electrodes 2.3 kN.[56]

3.1.4 Reinforcing mesh for integration into the concrete sample

Due to the fact that the automatic reinforcing mechanism and the contact welding machine were quite heavy (exceeding the maximum load capacity of the gantry robot used as the printhead motion system), and also a three-phase power source was required for the contact welding machine, for safety reasons it was decided to make the reinforcing mesh separately from the 3D printing of concrete in the test (departing from the concept). Due to the X-ray camera's 100 mm working area width, it was decided to use only one row of reinforcing mesh instead of two.

The reinforcing mesh was made on the automatic reinforcing mechanism in automatic mode with one exception: horizontal reinforcement was loaded manually, since the automatic reinforcing mechanism was not yet installed on a construction 3D printer.

The reinforcing mesh consists of two rows of vertical (each 80 mm long) and horizontal reinforcements (each 530 mm long) on top of each other (Fig. S1). Vertical reinforcements are welded to horizontal reinforcements in a checkerboard pattern. Since the printed sample consists of only 3 layers, the third row of vertical reinforcements was not needed.

3.2 Integration of the reinforcement mesh into the concrete

3.2.1 Nozzle design

In order to reinforce the printed concrete during the printing process it is necessary to solve the following challenges: (1) The created reinforcement meshes described in Paragraph 3.1 must be placed inside the printed concrete in one, two or more rows (in the proposed concept, two rows) at a certain distance A and B from the outer wall of the concrete layer and between each other, respectively (Fig. 4A). (2) The upper part of the vertical reinforcement bar should pass through the nozzle, dry and clean, for the subsequent contact welding with the horizontal reinforcement of the next layer. (3) The reinforcement mesh placed inside the printed concrete layer should be well integrated into the concrete (Fig. 4B).

Previous works partially solved these problems for

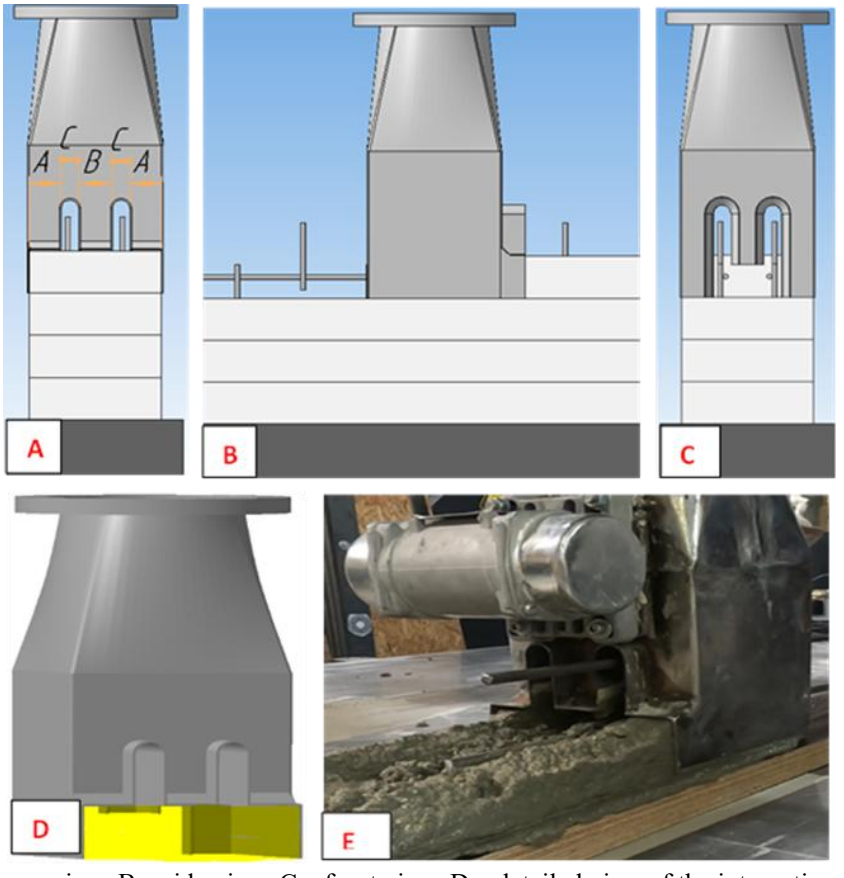

Fig. 4: Nozzle design: A – rear view, B – side view, C – front view, D – detailed view of the integration zone (marked in yellow), E – vibrator (Moser, 500 N at 50 Hz) mounted on the nozzle.

single-row metal mesh (29) and by the Chinese company Huashang Tengda for single-row reinforcement mesh of 1.5 meters height (48). Both cases used a split nozzle, *i.e.* in the center of the nozzle there was a hole (tunnel type) for the passage of metal/reinforcement mesh. Both have their drawbacks; the metal mesh was too small, so the authors switched to reinforcing 3D printed concrete with vertical reinforcement bars (49). And Huashang Tengda used pre-installed reinforcement meshes, which were produced manually.

The reinforcement meshes must be placed at such a distance from the outside of the wall that the risk of corrosion is minimised. According to the regulations, this should be at least 20 mm from the outside of the wall (depending on the exposure class).[57] Furthermore, the reinforcement meshes must be positioned in a way that the concrete can flow unhindered through the centre hole of the nozzle. For this purpose, a nozzle with two vertical passages was designed, through which the two rows of reinforcement mesh can pass (Fig. 4A). The design principles are as follows: The width of the openings to pass the welded bars should be equal to the sum of the diameters of the vertical and horizontal bars (dv, dh) plus a safety distance 'b' on the two sides C = dh + dv + 2b. The width of the printed layer is 150 mm in order to comply with the CONPrint3D concept.[58] This layer width allows standard reinforcement in two parallel rows. In the front part of the nozzle, where the opening starts, a chamber has been provided for an easy passage of the reinforcement mesh, even if the meshes are slightly inclined, they will pass through the nozzle (Fig. 4C). The integration of the reinforcement mesh is shown in Fig. 4E. To improve the integration of the reinforcement in concrete, the required concrete flow is increased by a few percent above the theoretically required value. An additional vibrator (Moser, 500 N at 50 Hz) is integrated at the rear of the nozzle (Fig. 4E). The vibration improves the flowability of the concrete during extrusion.[59] The concrete can emerge evenly at all three nozzle openings and blocking is prevented. The integration zone, as shown in Figs. 4D and 4E, is the lower undivided part of the nozzle. The extruded concrete is forced by the extrusion pressure and the rigid outer walls to fill all cavities in the integration zone. The integration zone is as high as the layer height so that the concrete can flow unhindered around the horizontal reinforcement and cannot touch the upper area of the vertical reinforcement because the opening C in Fig. 4 is designed like a tunnel.

The integration zone is very important because ignoring it will lead to a significant deterioration of the integration of the reinforcement into the concrete. Classen *et al*. used a printhead where several seperate nozzles were embedded in a row with no common integration zone. The result is a poor reinforcement integration into the concrete.[53,54]

3.2.2 Sample 3D printing

Before printing, one row of reinforcing mesh was installed on a wooden base (Fig. S2A). A gantry robot with a working area of 2x1x2 meters was used for 3D printing. The sample was printed in 3 layers at a print speed of 83 mm/s. The first layer of concrete was printed on a wooden base to remove the sample from the test bench for the X-ray scan. However, the height of the wooden base was not high enough to affect the experiment, and it was compensated by increasing the starting height of the printhead. This wooden foundation fixes the reinforcement during the printing process. But the reinforcement has been manually placed before printing. After printing the first layer, the lower horizontal reinforcement was integrated into the concrete by half, that is, the upper part of the lower horizontal reinforcement bar was not covered by concrete (Fig. S2B). The second layer was printed over the first layer. After printing the second layer, the lower horizontal reinforcing bar was fully integrated into the concrete and the upper horizontal reinforcing bar protruded dry over the second layer (Fig. S2C). In order to deliberately disrupt the integration zone, a part of the sample width (1/3 of the layer width) was carefully removed with a trowel in the soft state of the concrete before printing the third layer, without affecting the integrity and shape of the sample in any way (Fig. S2D). Because of this, during the printing of the third layer, part of the concrete fell down and the integration zone was disrupted (Fig. S2E).The printed sample was left to cure in a closed air-conditioned room at room temperature (24°C and humidity 50% for 7 days.)

3.2.3 X-ray scanning of the sample

An X-ray scanner (model: diondo d2) was used to check the integration of the reinforcement mesh into the concrete in an undamaged condition. In Fig.5, the sample is rotatably supported in the working area (40x40x70 cm). The sample is then scanned layer by layer from three orthogonal directions. The scanned images are combined to form a 3D model. The resolution is 1 µm.

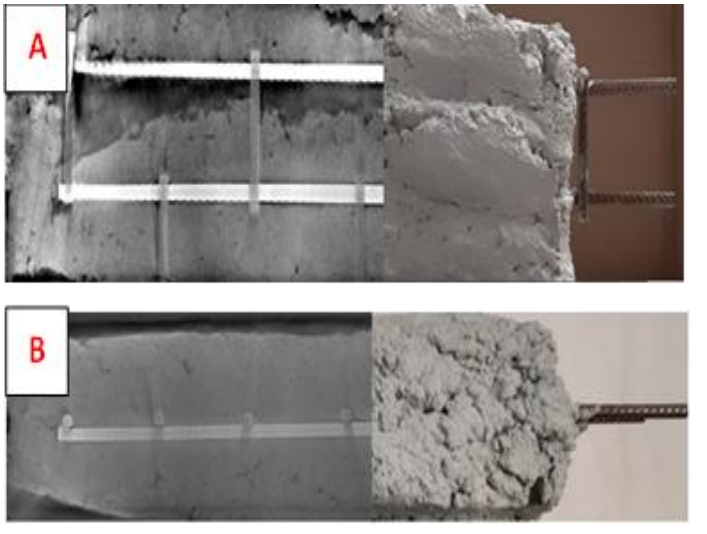

Fig. 5: X-ray scanning of the sample: A – Sideview, B – Top view, Lower bar (left section: X-ray scan, right section: photo).

3.2.4 Cutting of the sample

To be able to evaluate the sample in different cross-sections, it should be cut in several pieces perpendicular to the printing direction. To prevent the loosening of reinforcing bars due to vibrations caused by sawing, the sample was first sealed with plaster and filled with wax. After the wax hardened, the sample was cut perpendicular into seven parts and numbered (Fig. S3A). So, two numbers show the same cut. This allows for the evaluation of integration along vertical reinforcements. After that, selectively, some parts were cut in the direction of printing in order to evaluate the integration along the horizontal reinforcements (Figs. S3B and C).

4. Results and discussion

4.1 Shear test results for welded joints of crossed reinforcement bars

Table 2 shows the results of tests for shearing crossed reinforcing bars with a diameter of 8 mm in various combinations relative to each other: rib to rib, pocket to pocket, rib to pocket, edge to edge (see Fig. 3). The test results showed that it is possible to achieve the shear force required by the DIN 488-4 standard, which sets a minimum shear force of 6.28 kN for crossed reinforcing bars with a diameter of 8 mm. Scotchmer *et al*. note the main parameters affecting the strength of the contact weld are current, welding time and electrode crimping force.[60] According to this work, the minimum current for cross-shaped reinforcing bars with diameters of 8 mm should be higher than 5kA. The electrode crimping force (2,3 kN) and welding time (0,3 s), the welding current is given in Table 2.

The data in Table 2 are graphically illustrated in Fig. 6, which shows that some of the results do not reach the required strength (in Fig. 6, the minimum shear load defined by DIN 488-4 is indicated by a dotted line.). The failure rate for all 20 examples is 55%. It is noticeable that early failure occurs more often in “rib-rib” combinations (80%), “pocket-pocket” and “rib-pocket” combinations (60%), and the lowest failure rate in the “edge-edge” combination (20%).

The reasons for early failures in "rib-rib" combinations may be the small contact area during welding (Fig. 7A). This results in a small area of the welding zone due to the limited welding time. In the case of "pocket-pocket" and "rib-pocket" combinations, the cause of early failures may be the appearance of several contact points (Figs. 7B and C), parallel to each other from the point of view of the electrical circuit. Therefore, the current is divided according to the resistance and the number of contact points. This means that the welding current is lower at each contact point and the required welding temperature doesn’t reached. As a result, the weld point connection is defective and the knot force isn’t achieved. In the case of "edge-edge" combination, the risk of several points of contact is minimal, usually when the edge of a vertical bar touches the edge of a horizontal bar, it looks like two rectangles touching perpendicular to each other (Fig. 7D), respectively, in most cases, the welded contact point is solid and the contact area is large enough. Therefore, the probability to withstand the required minimum load is higher.

Another reason for early failure may be insufficient

Table 2: Shear test results for 8mm crossed reinforcing bars.

No	Bar orientation							
	edge – edge		rib – pocket		pocket - pocket		rib - rib	
	Welding Current (measured) [kA]	Shear force (measured) [kN]	Welding Current (measured) [kA]	Shear force (measured) [kN]	Welding Current (measured) [kA]	Shear force (measured) [kN]	Welding Current (measured) [kA]	Shear force (measured) [kN]
1	5.60	7.70	4.80	5.23	5.40	3.03	5.50	5.87
2	5.50	6.04	4.90	5.74	5.50	7.29	5.60	5.13
3	5.40	7.43	5.40	5.81	5.60	6.98	5.30	5.47
4	4.90	6.70	5.60	8.20	5.50	5.29	5.50	6.10
5	4.80	6.47	5.40	7.26	5.50	6.24	5.40	6.34

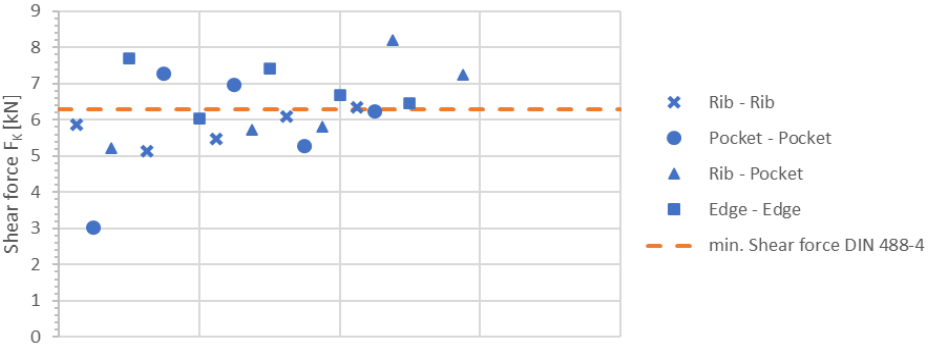

Fig. 6: Shear test results for 8 mm crossed bar connections.

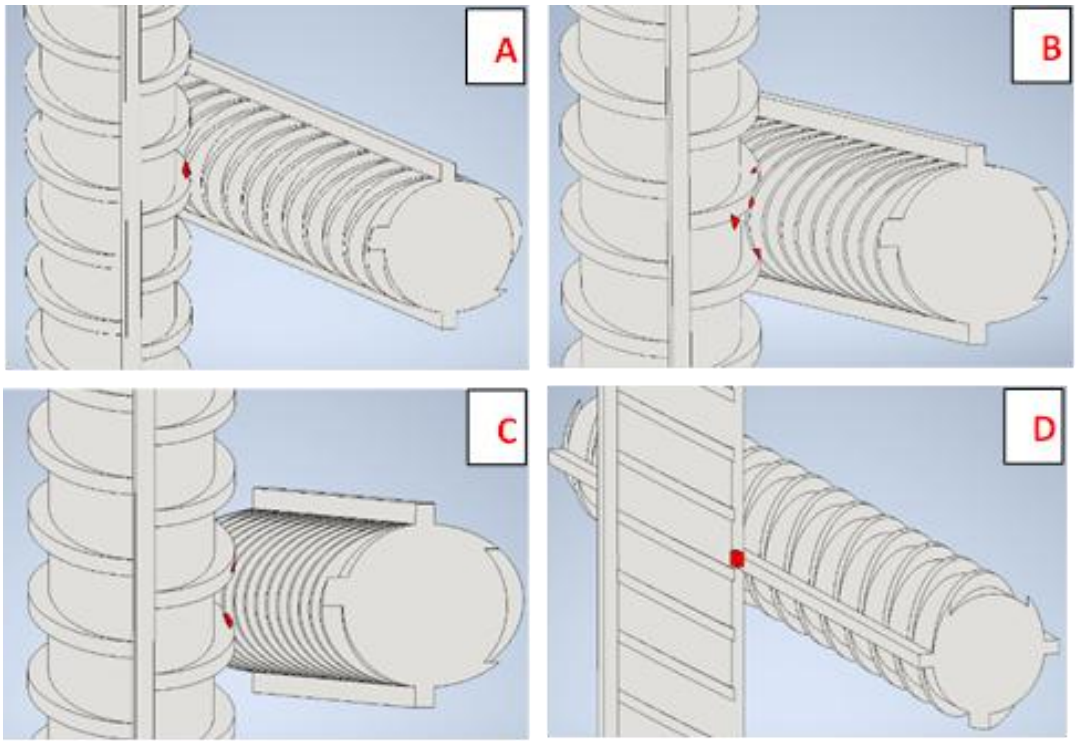

Fig. 7: The location of reinforcing bars relative to each other in various combinations and the contact zone (marked in red) at the beginning of resistance spot welding: A – rib-rib; B – pocket-pocket, C – rib-pocket; D – edge-edge.

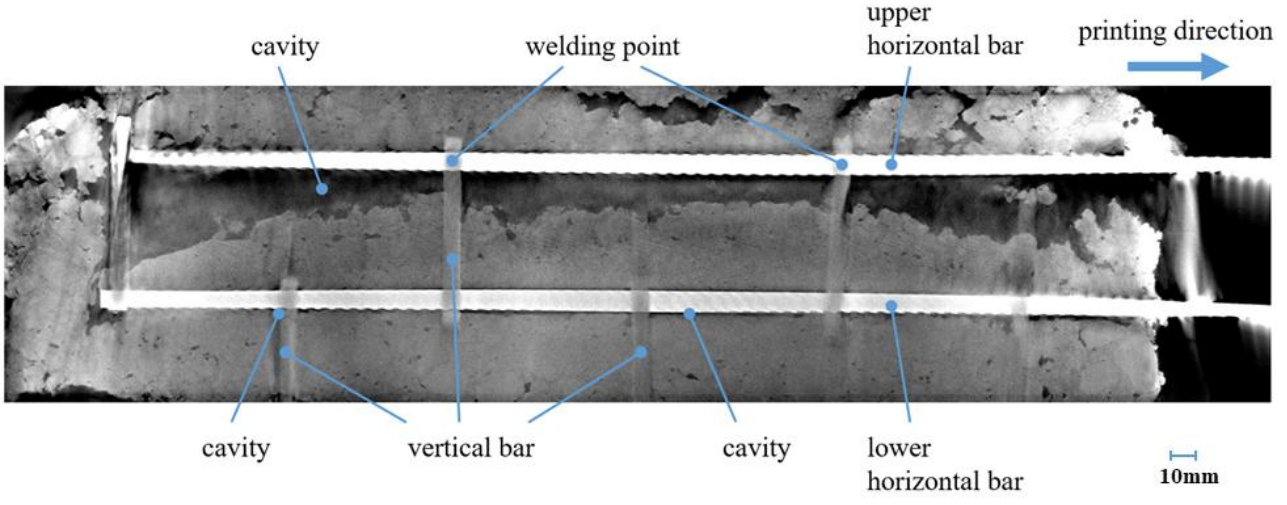

Fig. 8: Results of X-ray scanning of the sample.

electrode crimping force and welding current. The literature recommends the following parameters for 8 mm diameter reinforcing bars for good strength of the weld: electrode crimping force 3 kN, welding current 7.6 kA.[60] These parameters are more than the figures chosen in the test described here, where the welding current was from 4.8 kA to 5.6 kA and the electrode crimping force was 2.3 kN. The test results show that these parameters are sufficient for edge-to-edge combination, but there is a need to install an additional device in the automatic reinforcing mechanism, which will align the vertical and horizontal reinforcing bars so that the edge-to-edge combination is strictly observed at the welding point. An alternative solution may be to increase the electrode crimping force and welding current, which entails an increase in the power of the welding generator, respectively, an increase in its weight. Hence the conclusion: either it is necessary to accept an increase of the total mass of the printhead and install a more powerful welding generator, or it is necessary to lighten the mass by using a less powerful welding generator and adding a device for securing a defined orientation of the vertical and horizontal reinforcing bars. The other alternative is to increase the crimping force during the welding process. It should be noted here that the frame of the reinforcement integrator is stiffened in order to withstand the stresses that occur. This can also lead to an increase in the weight of the print head, but this is estimated to be less than

the increase in weight due to a larger generator.

The potential of the proposed concept is encouraging and can be assessed by its performance. In order for the sample to have a sufficient number of welded joints for the experiment, the distance between the vertical reinforcement bars was chosen to be 75/150 mm and between the horizontal 50 mm, respectively, the productivity of 3D printing of the wall according to the given conditions is about 14 m^2 per hour. This is less than that of AMoRC, where the productivity, as the authors claim, is 28 m^2 per hour.[54] However, if the reinforcement meshes are fabricated in the same manner as those of AMoRC 250 mm x 250 mm, positioned between the vertical and horizontal reinforcement, the speed of creating the reinforcement mesh will increase by more than three times. Consequently, the productivity of 3D printing the wall will be at least 42 m^2 per hour. The reinforcing mechanism can provide such speeds of creating the reinforcement mesh. Only the height of the hole in the nozzle will need to be increased accordingly to the height of the vertical reinforcement bar.

4.2 Results of X-ray scanning of the sample

The results of the X-ray scanning are shown in Fig. 8. The integration of the reinforcement grid is better in the lower layers than in the upper layers. Fig. 8 shows large cavities below the upper horizontal reinforcement. These cavities were caused by a disturbance in the integration zone. Consequently, the concrete could not flow properly under the upper horizontal reinforcement as no pressure was created in the integration zone for this purpose.

The material was removed in order to limit the mass of the final sample, as the load-bearing capacity of the CT scanner's sample holder is limited. This variant was chosen because the hardened sample should not be cut before the scan in order to avoid loosening the reinforcement from the concrete due to vibration during the cutting process.

Furthermore, Fig. 8 shows smaller cavities at the joints of the horizontal and vertical reinforcement and along the underside of the lower horizontal bar. One reason for this is the flow direction of the material. The nozzle tends to press the material onto the reinforcement from above, so that the cavities occur on the side facing away from the flow-around reinforcement (slipstream side). 3D concrete printing typically uses a rather stiff material consistency, as the material should hold the strand shape after it has been deposited. This lower flowability also makes it more difficult for concrete to flow around the reinforcement. To compensate for unevenness in the print bed, the nozzle had to print the first layer at a distance from the floor. This led to concrete escaping from the integration zone, which reduced the concrete pressure in the integration zone.

In Fig. 8, the lower bar shows that the cavities are more pronounced at both ends of the sample. The reason for this may be that not enough material was introduced into the integration zone when the printhead stands still. Likewise, due to a missing boundary on the back of the nozzle at the beginning of the printing process, it is not possible to generate the required concrete pressure in the integration zone, as the material exits to the rear instead of enclosing the reinforcement.

4.3 The Results of the cutting test

4.3.1 The results of tests for a cut in the direction perpendicular to the printing direction

The results of tests for a cut in the direction perpendicular to the printing direction are shown in Fig. S4. In the cross section, there is a clear tendency for cavities to appear near the lower horizontal reinforcement: from 2a to 4a cavities appear (Fig. S4), from 4a to 7a cavities appear absent (Fig. S4). This is explained by the fact that when printing the first layer at the beginning of the layer, the concrete pressure in the integration zone was insufficient due to the lack of a limiter at the rear of the nozzle. Therefore, cavities around the lower horizontal reinforcement appear at the beginning of printing and disappear towards the center of the sample when the concrete pressure reaches a sufficient level. The size of the cavity around the top horizontal reinforcement decreases from the edge of the sample (Fig. S4-1b) to the centre (Fig. S4-4b-5b,) and then increases again (Fig. S4-7a). This can be explained by the beginning and end of the printing process as explained. Although in this case of the 3rd layer printing the integration zone was deliberately disrupted, the beginning and end of the printing process had an additional impact, leading to a result where the cavities are larger at both ends than in the middle.

If the concrete pressure is at a sufficient level, the vertical reinforcement is well encased in concrete. The Fig. S4-3a shows good integration of the lower part of the vertical reinforcement, which coincides with the level of the first layer when the concrete pressure in the integration zone was sufficient.

4.3.2 The results of tests for a cut in the printing direction

The results of the cut in the printing direction tests confirmed the results of the previously described tests. Fig. S5 shows that in all cases, larger cavities are present in the lower part of the upper horizontal reinforcement. In section 6a-r, large cavities are present around the vertical reinforcement. This is explained by the start of printing. Small cavities below the lower horizontal reinforcement can be seen in the sectional views (Fig. S5-3a-r, 6a-1 and 7a-1), particularly where larger aggregate is in direct contact with the reinforcement (Fig. S5-3a-r). If we consider that these cavities appeared in the first layer and where the concrete pressure in the integration zone was sufficient, then there is a risk of cavities occurring if there is large gravel under the horizontal reinforcement.

The solution to this problem can be either to increase the pressure of the concrete, but then there is a risk of concrete leaking into the side of the opening in the nozzle for passing the upper part of the vertical reinforcements; or provide a source of vibration for the integration zone to improve the flow of concrete so that the concrete can fill all cavities.[59]

5. Conclusion

This paper proposes the concept of creating a reinforcement mesh from standard ribbed steel reinforcement using an automatic reinforcing mechanism and integrating it into concrete during 3D printing. For this purpose, the strength of the contact point of vertical and horizontal reinforcing bars according to DIN 488-4. The quality of integration of the reinforcement mesh into concrete by X-ray scanning and cutting the 3D printed specimen perpendicular to the printing direction and in line with the printing direction is tested. The creation of reinforcement mesh from standard ribbed steel reinforcement using contact welding in automatic mode is feasible, and achieving the required strength of reinforcement meshes according to DIN 488-4 appears possible, even though not all tests conducted here met this standard. Full integration of reinforcement meshes during 3D printing can be achieved if the nozzle has a carefully designed integration zone and maintains sufficient concrete pressure within this zone. To ensure an even distribution of concrete around the reinforcing bars, especially when increasing the diameter of reinforcement bars and using coarse-grained concrete, additional measures such as a vibration excitation in the integration zone may be necessary. Furthermore, maintaining adequate concrete pressure throughout the entire printing process is crucial, necessitating improvements in the nozzle design to sustain the required pressure from start to finish. This work demonstrates the feasibility of creating a reinforcing mesh from standard steel reinforcing bars and integrating it into concrete during 3D printing, thereby establishing a foundation for further research. Future research should investigate the possibility of creating a reinforcing mesh (frame) from standard steel reinforcement bars connected in three directions to each other as is done in traditional reinforced concrete structures. Additionally, solving the problem with vertical reinforcement is necessary to maintain its strength characteristics for tensile forces.

Acknowledgments

This work is supported by the grant "AP19679899 – Research and development of a manipulator that compensates for deviations of a construction 3D printer based on a concrete pump truck and positioning the PrintHead" (2023-2025) of the Ministry of Education and Science Kazakhstan.

Conflict of Interest

There is no conflict of interest.

Supporting Information

Applicable.

References

[1] G. H. Ahmed, N. H. Askandar, G. B. Jumaa, A review of large-scale 3DCP: Material characteristics, mix design, printing process, and reinforcement strategies, *Structures*, 2022, **43**, 508-532, doi: 10.1016/j.istruc.2022.06.068.

[2] F. Craveiro, S. Nazarian, H. Bartolo, P. J. Bartolo, J. Pinto Duarte, An automated system for 3D printing functionally graded concrete-based materials, *Additive Manufacturing*, 2020, **33**, 101146, doi: 10.1016/j.addma.2020.101146.

[3] Y.-C. Wu, M. Li, Effects of Early-Age rheology and printing time interval on Late-Age fracture characteristics of 3D printed concrete, *Construction and Building Materials*, 2022, **351**, 128559, doi: 10.1016/j.conbuildmat.2022.128559.

[4] Y. Wu, C. Liu, H. Liu, Z. Zhang, C. He, S. Liu, R. Zhang, Y. Wang, G. Bai, Study on the rheology and buildability of 3D printed concrete with recycled coarse aggregates, *Journal of Building Engineering*, 2021, **42**, 103030, doi: 10.1016/j.jobe.2021.103030.

[5] M. T. Souza, I. M. Ferreira, E. Guzi de Moraes, L. Senff, A. P. Novaes de Oliveira, 3D printed concrete for large-scale buildings: an overview of rheology, printing parameters, chemical admixtures, reinforcements, and economic and environmental prospects, *Journal of Building Engineering*, 2020, **32**, 101833, doi: 10.1016/j.jobe.2020.101833.

[6] T. T. Le, S. A. Austin, S. Lim, R. A. Buswell, A. G. F. Gibb, T. Thorpe, Mix design and fresh properties for high-performance printing concrete, *Materials and Structures*, 2012, **45**, 1221-1232, doi: 10.1617/s11527-012-9828-z.

[7] J. G. Sanjayan, B. Nematollahi, 3D concrete printing for construction applications, *3D Concrete Printing Technology*, 2019, 1-11, doi: 10.1016/b978-0-12-815481-6.00001-4.

[8] V. N. Nerella, M. Näther, A. Iqbal, M. Butler, V. Mechtcherine, Inline quantification of extrudability of cementitious materials for digital construction, *Cement and Concrete Composites*, 2019, **95**, 260-270, doi: 10.1016/j.cemconcomp.2018.09.015.

[9] R. A. Buswell, W. R. Leal de Silva, S. Z. Jones, J. Dirrenberger, 3D printing using concrete extrusion: a roadmap for research, *Cement and Concrete Research*, 2018, **112**, 37-49, doi: 10.1016/j.cemconres.2018.05.006.

[10] Y. W. D. Tay, G. H. A. Ting, Y. Qian, B. Panda, L. He, M. J. Tan, Time gap effect on bond strength of 3D-printed concrete, *Virtual and Physical Prototyping*, 2019, **14**, 104-113, doi: 10.1080/17452759.2018.1500420.

[11] J. G. Sanjayan, B. Nematollahi, M. Xia, T. Marchment, Effect of surface moisture on inter-layer strength of 3D printed concrete, *Construction and Building Materials*, 2018, **172**, 468-475, doi: 10.1016/j.conbuildmat.2018.03.232.

[12] T. Marchment, J. G. Sanjayan, B. Nematollahi, M. Xia, Interlayer strength of 3D printed concrete: Influencing factors and method of enhancing, in: 3D Concrete Printing Technology: *Construction and Building Applications*, 2019, 151-170, doi: 10.1016/B978-0-12-815481-6.00012-9.

[13] E. Hosseini, M. Zakertabrizi, A. H. Korayem, G. Xu, A novel method to enhance the interlayer bonding of 3D printing concrete: an experimental and computational investigation, *Cement and Concrete Composites*, 2019, **99**, 112-119, doi: 10.1016/j.cemconcomp.2019.03.008.

[14] E. Hosseini, M. Zakertabrizi, A. H. Korayem, G. Xu, A novel method to enhance the interlayer bonding of 3D printing concrete:

An experimental and computational investigation, *Cement and Concrete Composites*, 2019, **99**, 103-113, doi: 10.1016/j.cemconcomp.2019.03.008.
[15] Y. Han, Z. Yang, T. Ding, J. Xiao, Environmental and economic assessment on 3D printed buildings with recycled concrete, *Journal of Cleaner Production*, 2021, **278**, 123884, doi: 10.1016/j.jclepro.2020.123884.
[16] I. Agustí-Juan, F. Müller, N. Hack, T. Wangler, G. Habert, Potential benefits of digital fabrication for complex structures: Environmental assessment of a robotically fabricated concrete wall, *Journal of Cleaner Production*, 2017, **154**, 330-340, doi: 10.1016/j.jclepro.2017.04.002.
[17] T. Marchment, J. Sanjayan, Bond properties of reinforcing bar penetrations in 3D concrete printing, *Automation in Construction*, 2020, **120**, 103394, doi: 10.1016/j.autcon.2020.103394.
[18] F. Bos, Z. Ahmed, E. Jutinov, T. Salet, Experimental exploration of metal cable as reinforcement in 3D printed concrete, *Materials*, 2017, **10**, 1314, doi: 10.3390/ma10111314.
[19] J. H. Lim, B. Panda, Q.-C. Pham, Improving flexural characteristics of 3D printed geopolymer composites with in-process steel cable reinforcement, *Construction and Building Materials*, 2018, **178**, 32-41, doi: 10.1016/j.conbuildmat.2018.05.010.
[20] G. Ma, Z. Li, L. Wang, G. Bai, Micro-cable reinforced geopolymer composite for extrusion-based 3D printing, *Materials Letters*, 2019, **235**, 144-147, doi: 10.1016/j.matlet.2018.09.159.
[21] V. Mechtcherine, A. Michel, M. Liebscher, T. Schmeier, Extrusion-based additive manufacturing with carbon reinforced concrete: concept and feasibility study, *Materials*, 2020, **13**, 2568, doi: 10.3390/ma13112568.
[22] J. Xiao, Z. Chen, T. Ding, S. Zou, Bending behaviour of steel cable reinforced 3D printed concrete in the direction perpendicular to the interfaces, *Cement and Concrete Composites*, 2022, **125**, 104313, doi: 10.1016/j.cemconcomp.2021.104313.
[23] Z. Li, G. Ma, F. Wang, L. Wang, J. Sanjayan, Expansive cementitious materials to improve micro-cable reinforcement bond in 3D concrete printing, *Cement and Concrete Composites*, 2022, **125**, 104304, doi: 10.1016/j.cemconcomp.2021.104304.
[24] M. Hojati, A. M. Memari, M. Zahabi, Z. Wu, Z. Li, K. Park, S. Nazarian, J. P. Duarte, Barbed-wire reinforcement for 3D concrete printing, *Automation in Construction*, 2022, **141**, 104438, doi: 10.1016/j.autcon.2022.104438.
[25] X. Li, M. Newlands, R. Jones, Performance of a multi-layer aligned steel fibre reinforced concrete beam: a preliminary investigation towards 3D printing, *Case Studies in Construction Materials*, 2024, **21**, e03615, doi: 10.1016/j.cscm.2024.e03615.
[26] M. Chen, J. Li, T. Zhang, M. Zhang, 3D printability of recycled steel fibre-reinforced ultra-high performance concrete, *Construction and Building Materials*, 2025, **462**, 139877, doi: 10.1016/j.conbuildmat.2025.139877.
[27] A. Perrot, Y. Jacquet, D. Rangeard, E. Courteille, M. Sonebi, Nailing of layers: a promising way to reinforce concrete 3D printing structures, *Materials*, 2020, **13**, 1518, doi: 10.3390/ma13071518.
[28] L. Wang, G. Ma, T. Liu, R. Buswell, Z. Li, Interlayer reinforcement of 3D printed concrete by the in-process deposition of U-nails, *Cement and Concrete Research*, 2021, **148**, 106535, doi: 10.1016/j.cemconres.2021.106535.
[29] T. Marchment, J. Sanjayan, Mesh reinforcing method for 3D concrete printing, *Automation in Construction*, 2020, **109**, 102992, doi: 10.1016/j.autcon.2019.102992.
[30] X. Cao, S. Yu, D. Zheng, H. Cui, Nail planting to enhance the interface bonding strength in 3D printed concrete, *Automation in Construction*, 2022, **141**, 104392, doi: 10.1016/j.autcon.2022.104392.
[31] L. Hass, F. Bos, Bending and pull-out tests on a novel screw type reinforcement for extrusion-based 3D printed concrete, Second RILEM International Conference on Concrete and Digital Fabrication. Cham: Springer, 2020: 632-645, doi: 10.1007/978-3-030-49916-7_64.
[32] V. Mechtcherine, J. Grafe, V. N. Nerella, E. Spaniol, M. Hertel, U. Füssel, 3D-printed steel reinforcement for digital concrete construction–Manufacture, mechanical properties and bond behaviour, *Construction and Building Materials*, 2018, **179**, 125-137, doi: 10.1016/j.conbuildmat.2018.05.202.
[33] J. Müller, M. Grabowski, C. Müller, J. Hensel, J. Unglaub, K. Thiele, H. Kloft, K. Dilger, Design and parameter identification of wire and arc additively manufactured (WAAM) steel bars for use in construction, *Metals*, 2019, **9**, 725, doi: 10.3390/met9070725.
[34] T. Ding, F. Qin, J. Xiao, X. Chen, Z. Zuo, Experimental study on the bond behaviour between steel bars and 3D printed concrete, *Journal of Building Engineering*, 2022, **49**, 104105, doi: 10.1016/j.jobe.2022.104105.
[35] Z. Wang, L. Jia, Z. Deng, C. Zhang, Z. Zhang, C. Chen, J. Pan, Y. Zhang, Bond behavior between steel bars and 3D printed concrete: Effect of concrete rheological property, steel bar diameter and paste coating, *Construction and Building Materials*, 2022, **349**, 128708, doi: 10.1016/j.conbuildmat.2022.128708.
[36] A. Aramburu, I. Calderon-Uriszar-Aldaca, I. Puente, Bonding strength of steel rebars perpendicular to the hardened 3D-printed concrete layers, *Construction and Building Materials*, 2022, **340**, 127827, doi: 10.1016/j.conbuildmat.2022.127827.
[37] H. Kloft, M. Empelmann, N. Hack, E. Herrmann, D. Lowke, Reinforcement strategies for 3D-concrete-printing, *Civil Engineering Design*, 2020, **2**, 131-139, doi: 10.1002/cend.202000022.
[38] S. Engel, J. Hegger, M. Classen, Multimodal automated fabrication with concrete: case study and structural performance of ribbed CFRP-reinforced concrete ceilings, *Additive Manufacturing*, 2025, **101**, 104689, doi: 10.1016/j.addma.2025.104689.
[39] M. Liu, L. Wang, G. Ma, W. Li, Y. Zhou, U-type steel wire mesh for the flexural performance enhancement of 3D printed concrete: a novel reinforcing approach, *Materials Letters*, 2023, **331**, 133429, doi: 10.1016/j.matlet.2022.133429.

[40] M. T. Mollah, R. Comminal, W. R. Leal da Silva, B. Šeta, J. Spangenberg, Computational fluid dynamics modelling and experimental analysis of reinforcement bar integration in 3D concrete printing, *Cement and Concrete Research*, 2023, **173**, 107263, doi: 10.1016/j.cemconres.2023.107263.
[41] L. Gebhard, L. Esposito, C. Menna, J. Mata-Falcón, Inter-laboratory study on the influence of 3D concrete printing set-ups on the bond behaviour of various reinforcements, *Cement and Concrete Composites*, 2022, **133**, 104660, doi: 10.1016/j.cemconcomp.2022.104660.
[42] S. Du, F. Teng, Z. Zhuang, D. Zhang, M. Li, H. Li, Y. Weng, A BIM-enabled robot control system for automated integration between rebar reinforcement and 3D concrete printing, *Virtual and Physical Prototyping*, 2024, **19**, e2332423, doi: 10.1080/17452759.2024.2332423.
[43] B. Baz, G. Aouad, P. Leblond, O. Al-Mansouri, M. D'Hondt, S. Remond, Mechanical assessment of concrete–Steel bonding in 3D printed elements, *Construction and Building Materials*, 2020, **256**, 119457, doi: 10.1016/j.conbuildmat.2020.119457.
[44] L. Gebhard, J. Mata-Falcón, A. Anton, B. Dillenburger, W. Kaufmann, Structural behaviour of 3D printed concrete beams with various reinforcement strategies, *Engineering Structures*, 2021, **240**, 112380, doi: 10.1016/j.engstruct.2021.112380.
[45] D. Asprone, F. Auricchio, C. Menna, V. Mercuri, 3D printing of reinforced concrete elements: Technology and design approach, *Construction and Building Materials*, 2018, **165**, 218-231, doi: 10.1016/j.conbuildmat.2018.01.018.
[46] T. A. M. Salet, Z. Y. Ahmed, F. P. Bos, H. L. M. Laagland, Design of a 3D printed concrete bridge by testing, *Virtual and Physical Prototyping*, 2018, **13**, 222-236, doi: 10.1080/17452759.2018.1476064.
[47] L. Gebhard, J. Mata-Falcón, A. Iqbal, W. Kaufmann, Structural behaviour of post-installed reinforcement for 3D concrete printed shells–A case study on water tanks, *Construction and Building Materials*, 2023, **366**, 130163, doi: 10.1016/j.conbuildmat.2022.130163.
[48] V. Mechtcherine, R. Buswell, H. Kloft, F. P. Bos, N. Hack, R. Wolfs, J. Sanjayan, B. Nematollahi, E. Ivaniuk, T. Neef, Integrating reinforcement in digital fabrication with concrete: a review and classification framework, *Cement and Concrete Composites*, 2021, **119**, 103964, doi: 10.1016/j.cemconcomp.2021.103964.
[49] T. Marchment, J. Sanjayan, Reinforcement method for 3D concrete printing using paste-coated bar penetrations, *Automation in Construction*, 2021, **127**, 103694, doi: 10.1016/j.autcon.2021.103694.
[50] N. Freund, I. Dressler, D. Lowke, Studying the bond properties of vertical integrated short reinforcement in the shotcrete 3D printing process, Second RILEM International Conference on Concrete and Digital Fabrication. Cham: Springer, 2020: 612-621, doi: 10.1007/978-3-030-49916-7_62.
[51] C. Liu, Y. Zhang, H. Liu, Y. Wu, S. Yu, C. He, Z. Liang, Interlayer reinforced 3D printed concrete with recycled coarse aggregate: Shear properties and enhancement methods, *Additive Manufacturing*, 2024, **94**, 104507, doi: 10.1016/j.addma.2024.104507.
[52] N. Hack, K. Dörfler, A. N. Walzer, T. Wangler, J. Mata-Falcón, N. Kumar, J. Buchli, W. Kaufmann, R. J. Flatt, F. Gramazio, M. Kohler, Structural stay-in-place formwork for robotic *in situ* fabrication of non-standard concrete structures: a real scale architectural demonstrator, *Automation in Construction*, 2020, **115**, 103197, doi: 10.1016/j.autcon.2020.103197.
[53] M. Claßen, J. Claßen, R. Sharma, Konzeptionierung eines praxisorientierten 3D-druckverfahrens für den verbundwerkstoff stahlbeton (AMoRC), *Beton- und Stahlbetonbau*, 2020, **115**, 934-942, doi: 10.1002/best.202000023.
[54] M. Classen, J. Ungermann, R. Sharma, Additive manufacturing of reinforced concrete: development of a 3D printing technology for cementitious composites with metallic reinforcement, *Applied Sciences*, 2020, **10**, 3791, doi: 10.3390/app10113791.
[55] Y. Tao, M. K. Mohan, A. V. Rahul, G. De Schutter, K. Van Tittelboom, Influence of rheology on mixing homogeneity and mechanical behavior of twin-pipe 3D printable concrete, *Construction and Building Materials*, 2023, **408**, 133694, doi: 10.1016/j.conbuildmat.2023.133694.
[56] V. Mechtcherine, M. Taubert, S. Müller, F. Will, F. Storch, P. Plaschnick, J. Otto, P. Maiwald, 3D-gedruckte monolithische stahlbetonwände im CONPrint3D-reinforced verfahren, *Beton- und Stahlbetonbau*, 2022, **117**, 235-244, doi: 10.1002/best.202200001.
[57] C. Andrade, Propagation of reinforcement corrosion: principles, testing and modelling, *Materials and Structures*, 2019, **52**, 2.
[58] V. Mechtcherine, V. N. Nerella, F. Will, M. Näther, J. Otto, M. Krause, Large-scale digital concrete construction–CONPrint3D concept for on-site, monolithic 3D-printing, *Automation in Construction*, 2019, **107**, 102933, doi: 10.1016/j.autcon.2019.102933.
[59] F. Will, F. Storch, P. Plaschnick, M. Taubert, M. Butler, V. Mechtcherine, Large-scale monolithic printing with ready-mixed concrete: Challenges and solutions, *Digital Concrete 2024 – Supplementary Proceedings*, 2024, doi:10.24355/dbbs.084-202408150621-0.
[60] N. T. Williams, J. D. Parker, Review of resistance spot welding of steel sheets Part 2 Factors influencing electrode life, *International Materials Reviews*, 2004, **49**, 77-108.